nature geoscience

LETTERS

PUBLISHED ONLINE: 21 APRIL 2013 | DOI: 10.1038/NGEO1799

# Robust direct effect of carbon dioxide on tropical circulation and regional precipitation

Sandrine Bony[1]*, Gilles Bellon[2], Daniel Klocke[3], Steven Sherwood[4], Solange Fermepin[1] and Sébastien Denvil[1]

**Predicting the response of tropical rainfall to climate change remains a challenge[1]. Rising concentrations of carbon dioxide are expected to affect the hydrological cycle through increases in global mean temperature and the water vapour content of the atmosphere[2–4]. However, regional precipitation changes also closely depend on the atmospheric circulation, which is expected to weaken in a warmer world[4–6]. Here, we assess the effect of a rise in atmospheric carbon dioxide concentrations on tropical circulation and precipitation by analysing results from a suite of simulations from multiple state-of-the-art climate models, and an operational numerical weather prediction model. In a scenario in which humans continue to use fossil fuels unabated, about half the tropical circulation change projected by the end of the twenty-first century, and consequently a large fraction of the regional precipitation change, is independent of global surface warming. Instead, these robust circulation and precipitation changes are a consequence of the weaker net radiative cooling of the atmosphere associated with higher atmospheric carbon dioxide levels, which affects the strength of atmospheric vertical motions. This implies that geo-engineering schemes aimed at reducing global warming without removing carbon dioxide from the atmosphere would fail to fully mitigate precipitation changes in the tropics. Strategies that may help constrain rainfall projections are suggested.**

Human activities have raised the carbon dioxide ($CO_2$) concentration in the atmosphere, and further rise seems inevitable during the next decades. Difficulties in quantifying climate feedbacks[7] make the estimate of the global warming associated with increased $CO_2$ uncertain, and the estimate of regional precipitation changes induced by surface warming even more uncertain. These are of particular concern in the tropics where human welfare closely depends on rainfall. However, several studies have shown that $CO_2$ could also impact the atmosphere through fast adjustments independent of surface temperature changes[2,8]. How much, then, do regional precipitation changes projected by the end of the century depend on the surface warming?

We address this question by analysing a suite of numerical simulations from 16 state-of-the-art coupled ocean–atmosphere general circulation models (OAGCMs) participating in the Fifth Phase of the Coupled Models Inter-comparison Project (CMIP5; ref. 9, see Methods and Supplementary Information). Assuming a socio-economic pathway where humans continue to use fossil fuels with no mitigation (RCP8.5 scenario[10]), these models project by the end of the twenty-first century a tropical (30° S–30° N) mean surface warming relative to pre-industrial temperatures of 4.2 K (with a standard deviation of 1.1 K), larger over land than over ocean, and large changes in the regional distribution of rainfall ($\Delta P$, Fig. 1).

We interpret the response of tropical precipitation by dividing it into two components[4,11–14]: a dynamic one due to circulation changes, and one independent of these (see Methods). Using the vertically averaged large-scale vertical (pressure) air velocity $\bar{\omega}$ (defined positive for downward motions) as a proxy for large-scale atmospheric motions, we diagnose the dynamic component ($\Delta P_{\mathrm{dyn}}$) as the contribution to $\Delta P$ from changes in $\bar{\omega}$. The remaining change is referred to as the thermodynamic component, $\Delta P_{\mathrm{ther}}$, that is, $\Delta P = \Delta P_{\mathrm{dyn}} + \Delta P_{\mathrm{ther}}$.

The multi-model mean $\Delta P_{\mathrm{ther}}$ exhibits a wet-get-wetter, dry-get-drier regional pattern[4] (Fig. 1). This is primarily explained by the increase in atmospheric water vapour with temperature (following the Clausius–Clapeyron relationship), and the associated increase of moisture convergence in the moist, rising branches of the present-day tropical circulation and moisture divergence in the dry, subsidence regions (Supplementary Fig. S2). This pattern, which is also found in observed trends[15,16], is thus closely related to the climatological distribution of precipitation. In contrast, circulation changes lead to a more complex pattern of precipitation changes ($\Delta P_{\mathrm{dyn}}$), which explains a large part of the spread of regional precipitation projections amongst climate models (about 70% of the tropical-mean variance, Supplementary Fig. S8).

The radiative forcing achieved around 2090 in the RCP8.5 scenario is equivalent to that produced by a quadrupling of the pre-industrial $CO_2$ concentration ($4 \times CO_2$). To assess the relative influence of increased $CO_2$ versus surface warming on tropical precipitation changes, we analyse alternative experiments with the same models in which the atmospheric $CO_2$ concentration is abruptly quadrupled and then held fixed, instead of increasing progressively (see Methods). When warming in these alternative experiments reaches 4 K, simulated regional changes in rainfall are nearly identical to those forecast for 2090. This alternative scenario, however, enables us to isolate the roles of $CO_2$ and surface warming in producing these consistent patterns.

The multi-model mean evolution of $\Delta P_{\mathrm{ther}}$ and $\Delta P_{\mathrm{dyn}}$ as a function of surface warming (Fig. 2) shows that the wet-get-wetter, dry-get-drier pattern ($\Delta P_{\mathrm{ther}}$) is weak shortly after the $CO_2$ increase, when surface warming is still small ($\leq$1 K), and that it subsequently strengthens with further warming. In contrast, $\Delta P_{\mathrm{dyn}}$ exhibits a fast response to increased $CO_2$ associated with large regional anomalies: precipitation increases over most land regions (partly driven by the mass convergence induced by their fast surface warming relative to the oceans), over the equatorial eastern Pacific and over subtropical

[1]LMD/IPSL, CNRS, Université Pierre et Marie Curie, 75252 Paris, France, [2]CNRM/GAME, CNRS, Météo-France, 31057 Toulouse, France, [3]European Centre for Medium-Range Weather Forecasts, Reading RG2 9AX, UK, [4]CCRC and Centre of Excellence for Climate System Science, University of New South Wales, Sydney, New South Wales 2052, Australia. *e-mail: bony@lmd.jussieu.fr.

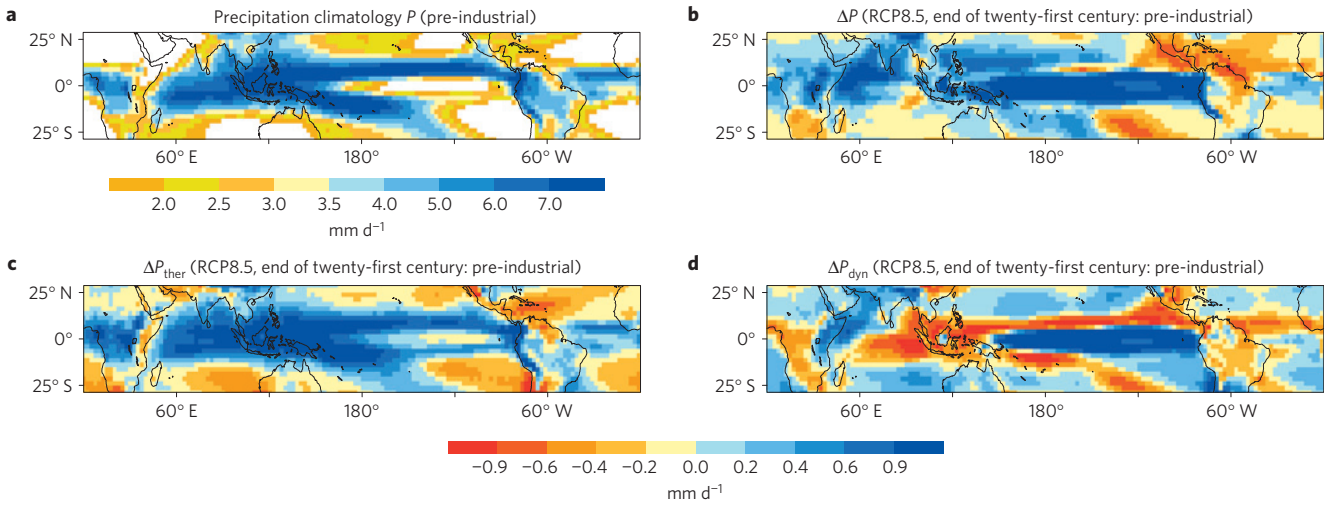


**Figure 1 | Multi-model mean projection of tropical precipitation changes at the end of the twenty-first century. a**, Climatological multi-model mean annual precipitation simulated by sixteen CMIP5 climate models in the pre-industrial climate. **b**–**d**, Multi-model mean change in annual precipitation (in mm d$^{-1}$) projected by the same models (**b**) and its decomposition ($\Delta P = \Delta P_{ther} + \Delta P_{dyn}$) into thermodynamic ($\Delta P_{ther}$; **c**) and dynamic ($\Delta P_{dyn}$; **d**) components at the end of the twenty-first century in a climate-change scenario without mitigation (RCP8.5).

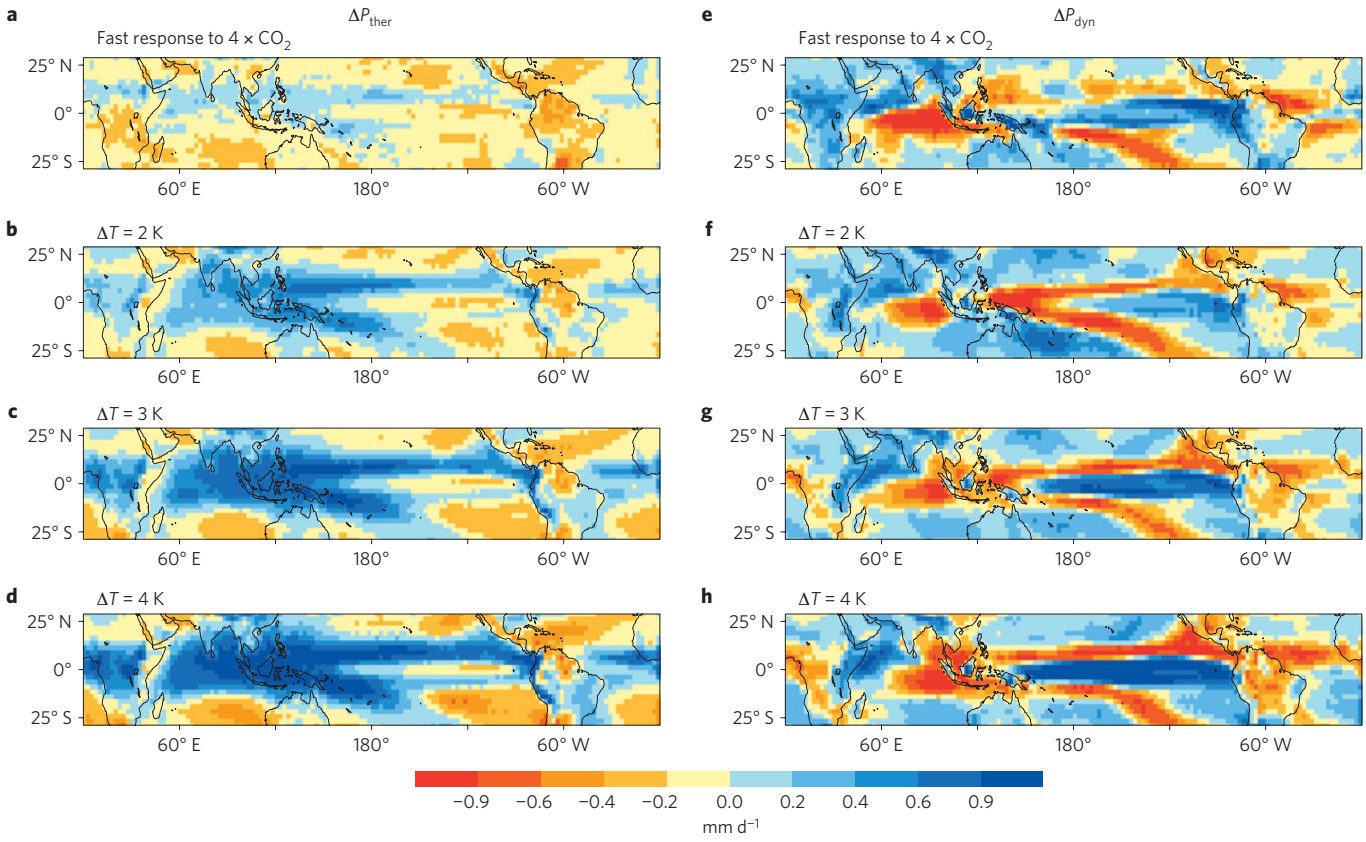


**Figure 2 | Interpretation of the multi-model mean regional pattern of tropical precipitation changes induced by a $CO_2$ increase. a**–**h**, Decomposition into thermodynamic ($\Delta P_{ther}$; **a**–**d**) and dynamic ($\Delta P_{dyn}$; **e**–**h**) components of the annual-mean precipitation change predicted by CMIP5 coupled ocean–atmosphere models at different stages of an experiment in which $CO_2$ is abruptly quadrupled: for the first year after $CO_2$ quadrupling (**a**,**e**), and for a tropical surface warming of 2 K (**b**,**f**), 3 K (**c**,**g**) and 4 K (**d**,**h**). Note the resemblance between the patterns simulated for a 4 K surface warming in this experiment and those projected by the end of the twenty-first century in the RCP 8.5 scenario (Fig. 1c,d).

dry regions, whereas it mostly decreases in regions of high present-day precipitation. Over land, $\Delta P_{dyn}$ weakens with surface warming in wet areas, and even changes sign in some regions (for example, central Africa and South America). Over ocean, on the contrary, $\Delta P_{dyn}$ evolves much less with surface warming, and the fast response pattern exhibits many similarities to the long-term pattern of $\Delta P_{dyn}$. It also forces an El Niño-like precipitation pattern.

To interpret the behaviour of $\Delta P_{dyn}$, we analyse the response of large-scale atmospheric vertical motions to increased $CO_2$ and surface warming. For this purpose, we compute the monthly average

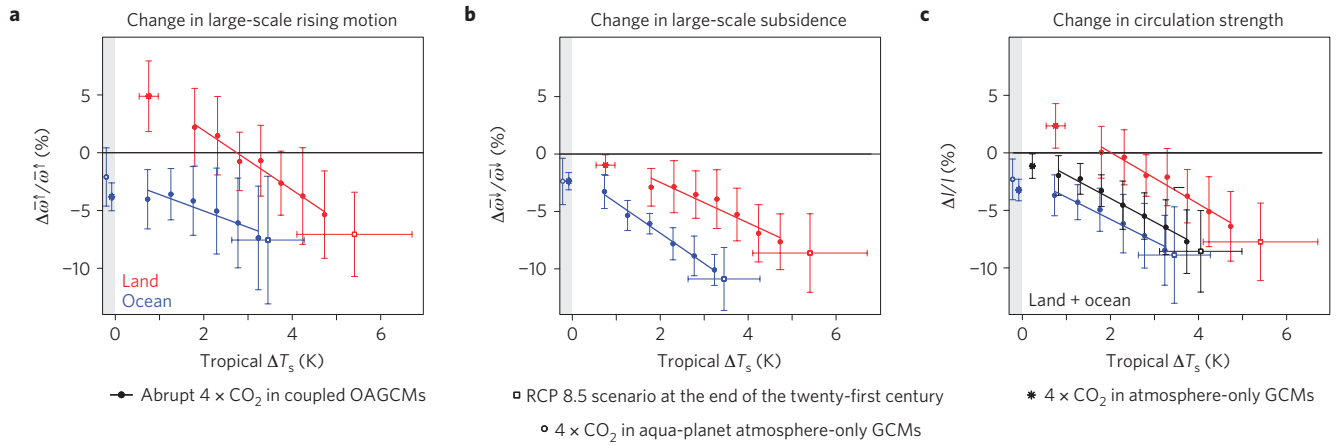


**Figure 3 | Response of the tropical atmospheric circulation to increased $CO_2$ in a range of CMIP5 experiments. a–c**, For land (red) and ocean (blue) areas, evolution with surface warming of the multi-model mean fractional change (compared with pre-industrial) in tropical-mean upward ($\bar{\omega}^{\uparrow}$; **a**) and downward ($\bar{\omega}^{\downarrow}$; **b**) vertical velocities, and in the strength of the overturning circulation ($I$; **c**) predicted by coupled ocean–atmosphere models after an abrupt $CO_2$ quadrupling (solid circles, shown only when at least 10 model results are available). Also reported are estimates from the non-mitigated RCP8.5 climate-change scenario around 2090 (open squares), and from 4 × $CO_2$ atmosphere-only experiments with fixed SSTs in realistic (stars) and aqua-planet (open circles) configurations. The vertical bars show ± 1 s.d. of individual model results around the multi-model mean.

upward ($\bar{\omega}^{\uparrow}$, negative) and downward ($\bar{\omega}^{\downarrow}$, positive) pressure vertical velocities for tropical land, ocean and land + ocean areas, as well as their difference $I = \bar{\omega}^{\downarrow} - \bar{\omega}^{\uparrow}$, which may be considered as a measure of the strength of the tropical overturning (or Hadley–Walker) circulation. In the pre-industrial climate, $\bar{\omega}^{\uparrow}$, $\bar{\omega}^{\downarrow}$ and $I_c$ are stable in time despite small (<2%) interannual fluctuations.

As climate warms, OAGCMs predict a progressive weakening of $\bar{\omega}^{\uparrow}$, $\bar{\omega}^{\downarrow}$ and $I_c$ over both land and ocean (Fig. 3). This is consistent with theories and numerical studies suggesting that the tropical circulation weakens under global warming owing to the increase in the lower-tropospheric water vapour and dry static stability of the atmosphere[4–6]. However, Fig. 3 also highlights a direct effect of increased $CO_2$ on the circulation: when surface warming is weak, the change in $CO_2$ induces a weakening of $\bar{\omega}^{\downarrow}$ over both land and ocean, a weakening of $\bar{\omega}^{\uparrow}$ over ocean, and a strengthening of $\bar{\omega}^{\uparrow}$ over land. This response occurs in every OAGCM examined, although with variable magnitude (Supplementary Table S2).

To confirm that these year-one changes are due mainly to $CO_2$ rather than the small amount of warming (≤1 K), and that they are robust, we examine further simulations where sea surface temperatures (SSTs) are held fixed during the $CO_2$ quadrupling, both in standard models and in versions with land removed (aqua-planets). With standard models, the responses of $\bar{\omega}^{\downarrow}$, $\bar{\omega}^{\uparrow}$ and $I_c$ to increased $CO_2$ are consistent with those predicted by OAGCMs during the first year (Fig. 3), and the aqua-planet responses account for a large fraction of those predicted with continents (more than 50% of rising motions changes, nearly 100% of subsidence changes and 70% of changes in circulation strength). The increased $CO_2$ thus exerts a direct effect on large-scale vertical motions that is not primarily mediated by surface temperature changes, nor by land–sea contrasts, although the latter amplify circulation changes.

This effect on the circulation explains much of the regional pattern of $\Delta P_{dyn}$ immediately after the abrupt $CO_2$ quadrupling (Fig. 2): over most land regions, precipitation increases owing to the strengthening of $\bar{\omega}^{\uparrow}$ and the weakening of $\bar{\omega}^{\downarrow}$; over ocean, precipitation increases in regions of present-day subsidence, and decreases in regions of present-day convection and high rain, consistently with the weakening of $\bar{\omega}^{\downarrow}$ and $\bar{\omega}^{\uparrow}$, respectively. Over ocean, comparing the impact on $\bar{\omega}^{\uparrow}$ of $CO_2$-alone versus that of $CO_2$ plus global warming (Fig. 3) shows that the direct effect of $CO_2$ explains about half of the weakening of large-scale ascent in the tropics simulated by climate models by the end of the century. Systematic changes in precipitation averaged over present-day wet and dry regions from direct $CO_2$ forcing are of comparable magnitude to those from warming (Supplementary Fig. S1).

How does $CO_2$ change the circulation? By reducing the loss of infrared radiation to space more than it affects the radiation at the surface, higher $CO_2$ concentrations weaken the net radiative cooling of the atmosphere. $CO_2$ thus exerts its direct effect by warming and slightly stabilizing the atmosphere, and by warming the continents relative to the oceans owing to the former's low heat capacity. Regional circulation responses on land are certainly sensitive to both[17,18]. However, the response of the overall overturning circulation is similar in models with and without continents (Fig. 3), indicating that it is driven mainly by the atmospheric heating.

To test this explanation, we run a single-column model (SCM) in the weak temperature gradient approximation[19], that is, in a configuration where the large-scale vertical velocity can be predicted for a range of SST values, given free-tropospheric temperatures that at low latitudes are fairly uniform (see Methods). The model qualitatively reproduces the subsidence over cooler SSTs and ascent over warmer SSTs seen in general circulation models (GCMs; Fig. 4). Moreover, when this model is rerun with 4 × $CO_2$ and the slightly warmer (hence, more stable) mean temperature profile simulated by the GCMs under this condition, it also reproduces the weakening of both descent and ascent (Fig. 4). Surface warming and land–sea contrasts are thus not the primary drivers of changes in the overturning circulation.

On what timescale does this dynamic adjustment occur? A climate model used in a numerical weather prediction mode[20] (see Methods) but forced by an abrupt $CO_2$ quadrupling shows that the circulation begins to change on the very first day, and that about half the 30-year mean change from 4 × $CO_2$ is achieved within only five days (Fig. 4). The $CO_2$ direct effect on circulation thus relies on fast physical processes. This calls for examining it in a GCM carefully evaluated on short timescales. For this purpose, we use the European Centre for Medium Range Weather Forecasts (ECMWF) Integrated Forecast System (IFS) operational model[21] and perform 10-day forecasts of the atmosphere for two months (October and April 2011) for 1 × $CO_2$ or 4 × $CO_2$ concentrations (see Methods). This model also predicts a fast circulation response over ocean (Fig. 4), and an enhancement of upward motions and precipitation over land (Supplementary Fig. S7). Over ocean, the weakening of

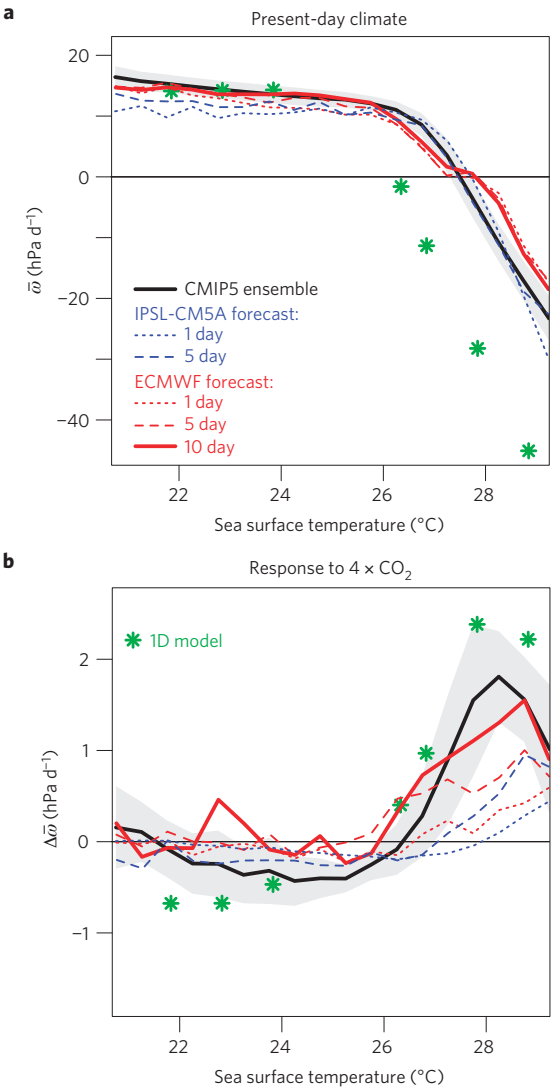


**Figure 4 | Interpretation and timescale of the direct effect of $CO_2$ on large-scale vertical motions. a**,**b**, Monthly mean $\bar{\omega}$ predicted by CMIP5 atmospheric GCMs over tropical oceans composited by SSTs in the present-day climate (**a**), and its change when atmospheric $CO_2$ is quadrupled but SSTs are kept unchanged ($4\times CO_2$–$1\times CO_2$; **b**). The black line shows multi-model mean values and the shaded area the inter-model standard deviation within each SST bin. Results from single-column (1D) simulations run in the weak temperature gradient approximation are shown by green stars. These simulations are compared with short atmospheric forecasts (at fixed forecast times) performed in $1\times CO_2$ and $4\times CO_2$ conditions using either a climate model (IPSL-CM5A) or an operational weather forecasting model (ECMWF).

upward motions occurs faster than that of subsidence. In convective areas associated with large-scale upward motions, the magnitude of the response after 10 days is comparable to that predicted on average over 30 years by CMIP5 atmospheric models.

The fast and direct effect of $CO_2$ on tropical vertical motions is thus physically understood and predicted by multiple climate models in a large spectrum of configurations and complexities. It is also predicted by a model that explicitly simulates individual cloud systems[22]. This robust result implies that part of the tropical precipitation response to climate change is independent of how much the surface warms. It also explains, for example, findings that geo-engineering options aiming at weakening global warming without removing $CO_2$ from the atmosphere would fail to fully mitigate precipitation changes at global or regional scales[23,24].

We conclude that regional precipitation responses to climate change are driven largely by physical mechanisms that are robust across climate models (Supplementary Information). So why do regional precipitation projections differ so much among models? Our study suggests at least three reasons. First, the correlation between $\Delta P_{\rm ther}$ and the precipitation climatology implies that model differences in the simulation of the present-day climate translate into different patterns of precipitation change (Supplementary Figs S3 and S4). Fortunately, observations of the former should help reduce uncertainty in the latter. Second, models still exhibit a large range of climate sensitivity estimates[25]. This alters the magnitude of $\Delta P_{\rm ther}$ relative to $\Delta P_{\rm dyn}$ and the sign of $\Delta P_{\rm dyn}$ over land, which adds uncertainty in the overall response (Fig. 2). Reducing the uncertainty in climate sensitivity will thus translate into a significant reduction of the precipitation projection uncertainty. Third, $\Delta P_{\rm dyn}$ is only partly constrained by the physical arguments explored here and exhibits significant variations between models, partly due to the $CO_2$-driven response (Supplementary Information). The latter being controlled by fast physical processes, however, supports the strategy of understanding it through process evaluations and weather-forecast simulations on very short timescales[20]. Such studies could also help constrain climate sensitivity estimates[8,25,26]. Therefore, long-standing uncertainties in climate projections may be decomposed into more tractable components, which may be more easily understood and constrained individually using climate and weather observations. Ultimately, this should help increase confidence in future climate-change assessments.

## Methods

**Atmospheric circulation diagnostics in CMIP5 models.** Monthly mean CMIP5 climate model outputs were retrieved from the Earth System Grid Federation archive (http://cmip-pcmdi.llnl.gov/cmip5). The list of CMIP5 models considered in this study is given in the Supplementary Information. We use single realizations of several CMIP5 experiments[9]: 30-year time slices of pre-industrial and abrupt $4\times CO_2$ coupled ocean–atmosphere experiments, 30-year atmosphere-only simulations forced by a fixed $1\times CO_2$ or $4\times CO_2$ concentration and using a prescribed SST distribution, 5-year aqua-planet experiments and 20-year time slices (2080–2099) of RCP8.5 experiments. For each CMIP5 simulation and model, we compute the vertical average $\bar{\omega}$ of pressure vertical velocity profiles, the probability distribution function $P_{\bar{\omega}}$ of $\bar{\omega}$ in the tropics[7] and the tropical-mean upward and downward vertical velocities over land, ocean and land + ocean regions.

**Dynamic and thermodynamic components of precipitation changes.** The monthly mean vertically integrated water budget is diagnosed at the regional scale for each model and each numerical experiment using (for example, ref. 27): $P = E - [q\vec{\nabla}\cdot\vec{V}] - [\vec{V}\cdot\vec{\nabla}q]$, where $P$ is the precipitation, $E$ is the surface evaporation, $\vec{V}$ is the horizontal wind and $q$ is the vertical profile of specific humidity. Brackets refer to mass-weighted vertical integrals. We note $H_q$ the vertically integrated horizontal moisture advection term ($-[\vec{V}.\vec{\nabla}q]$). Using mass continuity and after integration by parts over the depth of the troposphere, the term $-[q\vec{\nabla}.\vec{V}]$ is equal to $-[\omega\partial q/\partial\tilde{P}]$, where $\omega$ is the vertical profile of pressure vertical velocity and $\tilde{P}$ is the atmospheric pressure. As in the tropics the vertical structure of $\omega$ is close to a first baroclinic mode, we decompose $\omega$ as $\omega = \Omega + (\omega - \Omega)$, where $\Omega$ is a vertical velocity profile of vertically averaged value $\bar{\omega}$ and defined by $\Omega(\tilde{P}) = \bar{\omega}\,\Phi(\tilde{P})$. $\Phi$ is a specified vertical structure (a cubic polynomial vanishing at 1013 hPa and 100 hPa and having a maximum at 600 hPa, such that $\int_{100}^{1013}\Phi(\tilde{P})\,{\rm d}\tilde{P}/g = 1$, where $g$ is the gravitational acceleration). Then $P = E + \bar{\omega}\Gamma_q + V_q^{\alpha} + H_q$, with $\Gamma_q = -[\Phi(\tilde{P})(\partial q/\partial\tilde{P})]$ and $V_q^{\alpha} = -[(\omega(\tilde{P}) - \Omega(\tilde{P}))(\partial q/\partial\tilde{P})]$. The change in monthly mean precipitation can then be expressed as: $\Delta P = (\Delta E + \bar{\omega}\Delta\Gamma_q + \Delta H_q + \Delta V_q^{\alpha}) + \Gamma_q\Delta\bar{\omega} = \Delta P_{\rm ther} + \Delta P_{\rm dyn}$, with $\Delta P_{\rm dyn} = \Gamma_q\Delta\bar{\omega}$. The term $\Delta P_{\rm dyn}$ is referred to as the dynamic component because it is directly related to the change in $\bar{\omega}$. The other component, $\Delta P_{\rm ther}$, is referred to as the thermodynamic component because it is largely dominated by the Clausius–Clapeyron relationship (see Supplementary Information).

**SCM simulations.** SCM simulations of the tropical atmosphere in $1\times CO_2$ and $4\times CO_2$ conditions are performed with the IPSL-CM5A-LR atmospheric GCM (refs 28,29). In the weak temperature gradient approximation, justified by the weakness of horizontal temperature gradients in the tropical free troposphere, $\omega$ and its associated moisture convergence can be diagnosed from energy balance, given the

temperature profile[19]. In our set-up, the temperature profile of the SCM in the free troposphere (that is, at pressures lower than 800 hPa) is relaxed towards a specified tropical-mean temperature profile[30] derived from an atmospheric GCM (IPSL-CM5A-LR) simulation (in $1\times CO_2$ or $4\times CO_2$ conditions). Within the boundary layer, the vertical velocity is assumed to vary linearly with pressure and to vanish at the surface. Simulations are performed for $1\times CO_2$ and $4\times CO_2$ concentrations, for a range of SSTs and fixed surface wind (7 m $s^{-1}$, close to the tropical-mean value).

**Numerical weather prediction simulations.** Short-term simulations of the global atmosphere are performed for two values of the $CO_2$ concentration ($1\times CO_2$ or $4\times CO_2$) with two models: the atmospheric component[28] of the CMIP5 IPSL-CM5A-LR OAGCM (ref. 29) initialized with the ECMWF Year of Tropical Convection (YOTC, http://data-portal.ecmwf.int/data/d/yotc_od/) analysis data set for each day of January, April, July and October 2009 at 00 UTC, and the present version (CY37r2) of the ECMWF-IFS model initialized with its own corresponding analysis (at 00, 06, 12 and 18 UTC) for the months of April and October 2011. The ability of the ECMWF-IFS model to simulate fast physical processes is routinely assessed with two weather forecasts per day over several years[21]. For each month (in $1\times CO_2$ or $4\times CO_2$), we average the model outputs at fixed forecast times (1 day, 5 days and so on), and we stratify the regional monthly mean $\bar{\omega}$ by the monthly SST using 1 K bins.

Received 2 July 2012; accepted 12 March 2013; published online 21 April 2013

## References


1. Solomon, S. *et al.* in *Climate Change 2007: The Physical Science Basis* (eds Solomon, S. *et al.*) (Cambridge Univ. Press, 2007).
2. Mitchell, J. F. B. The seasonal response of a general circulation model to changes in $CO_2$ and sea temperatures. *Q. J. R. Meteorol. Soc.* **109,** 113–152 (1983).
3. Allen, M. R. & Ingram, W. J. Constraints on future changes in the hydrological cycle. *Nature* **419,** 224–228 (2002).
4. Held, I. M. & Soden, B. J. Robust responses of the hydrological cycle to global warming. *J. Clim.* **19,** 5686–5699 (2006).
5. Knutson, T. R. & Manabe, S. Time-mean response over the tropical Pacific to increased $CO_2$ in a coupled ocean–atmosphere model. *J. Clim.* **8,** 2181–2199 (1995).
6. Vecchi, G. A. & Soden, B. J. Global warming and the weakening of the tropical circulation. *J. Clim.* **20,** 4316–4340 (2007).
7. Bony, S. *et al.* How well do we understand and evaluate climate change feedback processes? *J. Clim.* **19,** 3445–3482 (2006).
8. Gregory, J. M. & Webb, M. J. Tropospheric adjustment induces a cloud component in $CO_2$ forcing. *J. Clim.* **21,** 58–71 (2008).
9. Taylor, K. E., Stouffer, R. J. & Meehl, G. A. An Overview of CMIP5 and the experiment design. *Bull. Am. Meteorol. Soc.* **93,** 485–498 (2012).
10. Moss, R. *et al.* A new approach to scenario development for the IPCC Fifth Assessment Report. *Nature* **463,** 747–756. (2010).
11. Emori, S. & Brown, S. J. Dynamic and thermodynamic changes in mean and extreme precipitation under changed climate. *Geophys. Res. Lett.* **32,** L17706 (2005).
12. Chou, C., Neelin, J. D., Chen, C-A. & Tu, J-Y. Evaluating the 'Rich-Get-Richer' mechanism in tropical precipitation change under global warming. *J. Clim.* **22,** 1982–2005 (2009).
13. Seager, R., Naik, N. & Vecchi, G. A. Thermodynamic and dynamic mechanisms for large-scale changes in the hydrological cycle in response to global warming. *J. Clim.* **23,** 4651–4668 (2010).
14. Muller, C. J. & O'Gorman, P. A. An energetic perspective on the regional response of precipitation to climate change. *Nature Clim. Change* **1,** 266–271 (2011).
15. Liu, C., Allan, R. P. & Huffman, G. J. Co-variation of temperature and precipitation in CMIP5 models and satellite observations. *Geophys. Res. Lett.* **39,** L13803 (2012).
16. Chou, C. *et al.* Increase in the range between wet and dry season precipitation. *Nature Geosci.* **6,** 263–267 (2013).
17. Joshi, M., Gregory, J., Webb, M., Sexton, D. & Johns, T. Mechanisms for the land-sea warming contrast exhibited by simulations of climate change. *Clim. Dynam.* **30,** 455–465 (2008).
18. Cao, L., Bala, G. & Caldeira, K. Climate response to changes in atmospheric carbon dioxide and solar irradiance on the timescale of days to weeks. *Environ. Res. Lett.* **7,** 034015 (2012).
19. Sobel, A. H. & Bretherton, C. S. Modelling tropical precipitation in a single column. *J. Clim.* **13,** 4378–4392 (2000).
20. Phillips, T. J. *et al.* Evaluating parameterizations in general circulation models: Climate simulation meets weather prediction. *Bull. Am. Meteorol. Soc.* **85,** 1903–1915 (2004).
21. Bechtold, P. *et al.* Advances in simulating atmospheric variability with the ECMWF model: From synoptic to decadal timescales. *Q. J. R Meteorol. Soc.* **134,** 1337–1351 (2008).
22. Wyant, M. C., Bretherton, C. S., Blossey, P. N. & Khairoutdinov, M. Fast cloud adjustment to increasing $CO_2$ in a superparameterized climate model. *JAMES* **4,** M05001 (2012).
23. Bala, G., Duffy, P. B. & Taylor, K. E. Impact of geoengineering schemes on the global hydrological cycle. *Proc. Natl Acad. Sci. USA* **105,** 7664–7669 (2008).
24. Schmidt, H. *et al.* Solar irradiance reduction to counteract radiative forcing from a quadrupling of $CO_2$: Climate responses simulated by four Earth System Models. *Earth Syst. Dynam.* **3,** 63–78 (2012).
25. Andrews, T., Gregory, J., Webb, M. & Taylor, K. Forcing, feedbacks and climate sensitivity in CMIP5 coupled atmosphere-ocean climate models. *Geophys. Res. Lett.* **39,** L09712 (2012).
26. Rodwell, M. & Palmer, T. N. Using numerical weather prediction to assess climate models. *Q. J. R. Meteorol. Soc.* **133,** 129–146 (2009).
27. Neelin, J. D. in *The Global Circulation of the Atmosphere* (eds Schneider, T. & Sobel, A.) 267–301 (Princeton Univ. Press, 2007).
28. Hourdin, F. *et al.* The LMDZ general circulation model: Climate performance and sensitivity to parameterized physics with emphasis on tropical convection. *Clim. Dynam.* **19,** 3445–3482 (2006).
29. Dufresne, J-L. *et al.* Climate change projections using the IPSL-CM5 Earth System Model: From CMIP3 to CMIP5. *Clim. Dynam.* http://dx.doi.org/10.1007/s00382-012-1636-1 (2013).
30. Raymond, D. J. & Zeng, X. Modelling tropical atmospheric convection in the context of the weak temperature gradient approximation. *Q. J. R. Meteorol. Soc.* **131,** 1301–1320 (2005).


## Acknowledgements

This work benefited from discussions with K. Emanuel, J-L. Dufresne, B. Stevens and T. Palmer, and from the technical help of J. Raciasek. The research leading to these results has received funding from the European Union, Seventh Framework Programme (FP7/2007-2013) under grant agreement no. 244067(EUCLIPSE), the French CEP&S 2010 ANR project ClimaConf and the LEFE project Missterre. We acknowledge the World Climate Research Programme's Working Group on Coupled Modelling, which is responsible for CMIP, and we thank the climate modelling groups (listed in the Supplementary Information) for producing and making available their model output. For CMIP the US Department of Energy's Program for Climate Model Diagnosis and Intercomparison provides coordinating support and led development of software infrastructure in partnership with the Global Organisation for Earth System Science Portals.

## Author contributions

S.B. designed the study and performed the analysis. S.B. and S.S. wrote the paper. D.K. designed and performed ECMWF forecasts and contributed to the graphics. G.B. designed and performed single-column simulations, S.F. designed and performed short-term IPSL simulations, S.D. organized the retrieval of CMIP5 model outputs. All authors discussed the results and edited the manuscript.

## Additional information

Supplementary information is available in the online version of the paper. Reprints and permissions information is available online at www.nature.com/reprints. Correspondence and requests for materials should be addressed to S.B.

## Competing financial interests

The authors declare no competing financial interests.